Universal Power Law Governing Pedestrian Interactions

Ioannis Karamouzas,[1] Brian Skinner,[2] and Stephen J. Guy[1]

[1]*Department of Computer Science and Engineering, University of Minnesota, Minneapolis, Minnesota 55455, USA*
[2]*Materials Science Division, Argonne National Laboratory, Argonne, Illinois 60439, USA*

Human crowds often bear a striking resemblance to interacting particle systems, and this has prompted many researchers to describe pedestrian dynamics in terms of interaction forces and potential energies. The correct quantitative form of this interaction, however, has remained an open question. Here, we introduce a novel statistical-mechanical approach to directly measure the interaction energy between pedestrians. This analysis, when applied to a large collection of human motion data, reveals a simple power-law interaction that is based not on the physical separation between pedestrians but on their projected time to a potential future collision, and is therefore fundamentally anticipatory in nature. Remarkably, this simple law is able to describe human interactions across a wide variety of situations, speeds, and densities. We further show, through simulations, that the interaction law we identify is sufficient to reproduce many known crowd phenomena.

In terms of its large-scale behaviors, a crowd of pedestrians can look strikingly similar to many other collections of repulsively interacting particles [1–4]. These similarities have inspired a variety of pedestrian crowd models, including cellular automata and continuum-based approaches [5–8], as well as simple particle or agent-based models [9–15]. Many of these models conform to a long-standing hypothesis that humans in a crowd interact with their neighbors through some form of "social potential" [16], analogous to the repulsive potential energies between physical particles. How to best determine the quantitative form of this interaction potential, however, has remained an open question, with most previous researchers employing a simulation-driven approach.

Previously, direct measurement of the interaction law between pedestrians has been confounded by two primary factors. First, each individual in a crowd experiences a complex environment of competing forces, making it difficult to isolate and robustly quantify a single pairwise interaction. Second, a pedestrian's motion is strongly influenced not just by the present position of neighboring pedestrians, but by their anticipated future positions [17–21], a fact which has influenced recent models [22–25]. Consider, for example, two well-separated pedestrians walking into a head-on collision [Fig. 1(a)]. These pedestrians typically exhibit relatively large acceleration as they move to avoid each other, as would result from a large repulsive force. On the other hand, pedestrians walking in parallel directions exhibit almost no acceleration, even when their mutual separation is small [Fig. 1(b)].

Here, we address both of the aforementioned factors using a data-driven, statistical mechanics-based analysis that accounts properly for the anticipatory nature of human interactions. This approach allows us to directly and robustly measure the interaction energy between pedestrians. The consistency of our measurements across a variety of settings suggests a simple and universal law governing pedestrian motion.

To perform our analysis, we turn to the large collections of recently published crowd data sets recorded by motion capture or computer vision-based techniques. These data sets include pedestrian trajectories from several outdoor environments [26,27] and controlled lab settings [28] (a summary of data sets is given in the Supplemental Material [29]). To reduce statistical noise, data sets with similar densities were combined together, resulting in one *Outdoor* data set comprising 1146 trajectories of pedestrians in sparse-to-moderate outdoor settings, and one *Bottleneck* data set with 354 trajectories of pedestrians in dense crowds passing through narrow bottlenecks. In analyzing these data sets, our primary tool for quantifying the strength of interactions between pedestrians is the statistical-mechanical pair distribution function, denoted g.

As in the typical condensed matter setting [35], here we define the pair distribution function $g(x)$ as the observed probability density for two pedestrians to have relative separation x divided by the expected probability density for two noninteracting pedestrians to have the same separation. In general, the probability density for noninteracting pedestrians cannot be known *a priori*, since it depends on where and how frequently pedestrians enter and exit the environment. However, for large data sets we are able to closely approximate this distribution by sampling the separation between all pairs of pedestrians that are not simultaneously present in the scene (and therefore not interacting). As defined above, small values of the pair distribution function, $g(x) \ll 1$, correspond to situations where interactions produce strong avoidance.
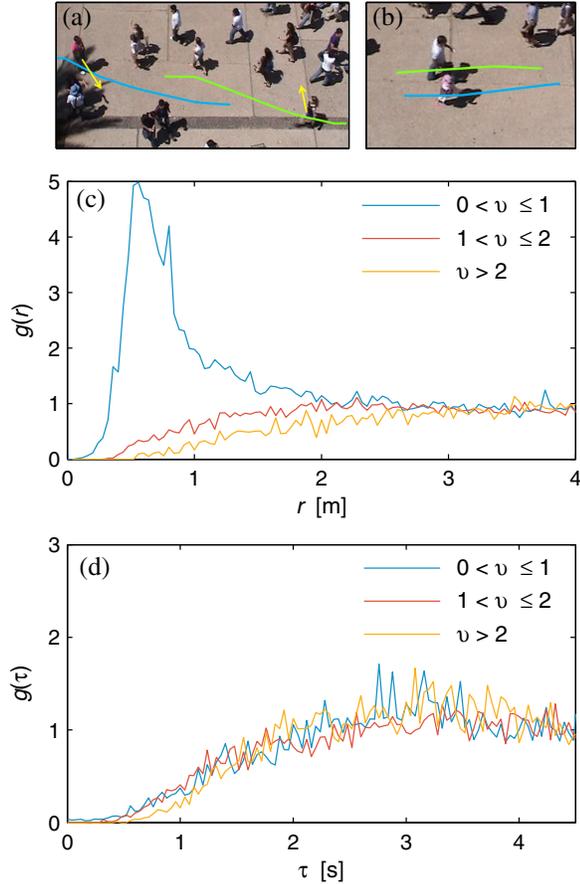
FIG. 1 (color online). Analysis of anticipation effects in pedestrian motion. (a) Two pedestrians react strongly to avoid an upcoming collision even though they are far from each other (path segments over an interval of 4s are shown as colored lines, with arrows indicating acceleration). (b) In the same environment, two pedestrians walk close to each other without any relative acceleration. (c) The pair distribution function g as a function of interpedestrian separation r shows very different behavior when plotted for pedestrian pairs with different rate of approach $v = -dr/dt$. Units of v are m/s. (d) In contrast, when g is computed as a function of the time to collision τ, curves corresponding to different v collapse onto each other.

If the Cartesian distance r between two pedestrians was a sufficient descriptor of their interaction, we would expect the shape of the pair distribution function $g(r)$ to be independent of all other variables. However, as can be seen in Fig. 1(c), $g(r)$ has large, qualitative differences when the data are binned by the rate at which the two pedestrians are approaching each other, $v = -dr/dt$. In particular, pedestrians with a small rate of approach are more likely to be found close together than those that are approaching each other quickly (as evidenced by the separation between the curves at small r). A particularly pronounced difference can be seen for the curve corresponding to small v, where the large peak suggests a tendency for pedestrians with similar velocities to walk closely together.

While the distance r is not a sufficient descriptor of interactions, we find that the pair distribution function can, in fact, be accurately parametrized by a single variable that describes how imminent potentially upcoming collisions are. We refer to this variable as the *time to collision*, denoted τ, which we define as the duration of time for which two pedestrians could continue walking at their current velocities before colliding. As shown in Fig. 1(d), when the pair distribution function is plotted as a function of τ, curves for different rates of approach collapse onto each other, with no evidence of a separate dependence of the interaction on v. Even when binned by other parameters such as the relative orientation between pedestrians, there is no significant difference between curves (see the Supplemental Material [29]). This consistent collapse of the curves suggests that the single variable τ provides an appropriate description of the interaction between pedestrians.

This pair distribution function $g(\tau)$ describes the extent to which different configurations of pedestrians are made unlikely by the mutual interaction between pedestrians. In general, situations with strong interactions (small τ) are suppressed statistically, since the mutual repulsion between two approaching pedestrians makes it very unlikely that the pedestrians will arrive at a situation where a collision is imminent. This suppression can be described in terms of a pedestrian "interaction energy" $E(\tau)$. In particular, in situations where the average density of pedestrians does not vary strongly with time, the probability of a pair of pedestrians having the time to collision τ can be assumed to follow a Boltzmann-like relation, $g(\tau) \propto \exp[-E(\tau)/E_0]$. Here, E_0 is a characteristic pedestrian energy, whose value is scene dependent.

This use of a Boltzmann-like relation between $g(\tau)$ and $E(\tau)$ amounts to an assumption that the systems being considered are at, or near, statistical equilibrium. In our analysis, this assumption is motivated by the observation that the intensive properties of the system in each of the data sets (e.g., the average pedestrian density and walking speed) are essentially time independent. If this time independence is taken as given, a Boltzmann-like relation follows as a consequence of entropy maximization. By rearranging this relation, the interaction energy can be expressed in terms of $g(\tau)$ as

$$E(\tau) \propto \ln\left[1/g(\tau)\right]. \qquad (1)$$

A further, self-consistent validation of Eq. (1) is provided below.

Figure 2 plots the interaction law defined by Eq. (1) using the values for $g(\tau)$ derived from our two aggregated pedestrian data sets. It is worth emphasizing that these two data sets capture very different types of pedestrian motion. The pedestrian trajectories in the Outdoor data set are generally multidirectional paths in sparse-to-moderate
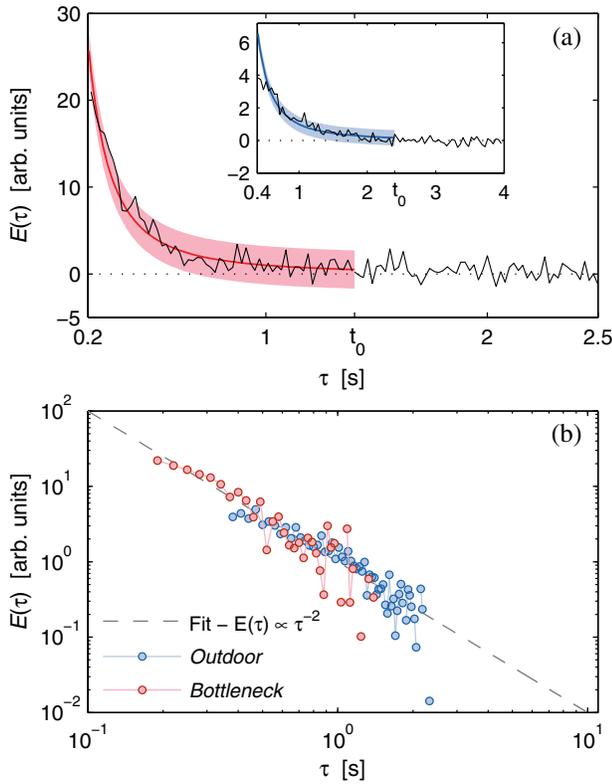
FIG. 2 (color online). (a) The interaction energy computed from the dense Bottleneck data set and from the more sparse Outdoor data set (inset). The overall constant k is normalized so that $E(1) = 1$. Both data sets fit well to a power law up to a point marked t_0, beyond which there is no discernible interaction. Solid lines show the fit to the data and colored regions show their corresponding 95% confidence interval (Bottleneck, $R^2 = 0.94$; Outdoor, $R^2 = 0.92$). (b) The interaction energy in both data sets is well described by a power law with exponent 2.

densities, with pedestrians often walking in groups or stopping for brief conversations. In contrast, trajectories in the Bottleneck data set are largely unidirectional, with uniformly high density, and with little stopping or grouping between individuals.

Remarkably, despite their large qualitative differences, both data sets reveal the same power-law relationship underlying pedestrian interactions. For both data sets, the interaction energy E shows a quadratic falloff as a function of τ, so that $E(\tau) \propto 1/\tau^2$ over the interval where E is well defined. For smaller values of τ (less than ∼200 ms), the energy seen in the data saturates to a maximum value, likely as a consequence of finite human reaction times. For sufficiently large values of τ, on the other hand, the observed interaction energy quickly vanishes, suggesting a truncation of the interaction when the time to collision is large. We denote the maximum observed interaction range as t_0 (Bottleneck: $t_0 \approx 1.4$ s; Outdoor: $t_0 \approx 2.4$ s).

Importantly, t_0 does not, by itself, indicate the intrinsic interaction range between pedestrians, since interactions between distant, non-neighboring pedestrians are screened

by the presence of nearest neighbors, as in other dense, interacting systems [35,36]. For a crowd with density ρ, the characteristic "screening time" can be expected to scale as the typical distance between nearest neighbors, $\rho^{-1/2}$, divided by the mean walking speed u. Such scaling is indeed consistent with the trend observed in our data, with the denser Bottleneck data set ($\rho = 2.5$ m^{-2}, $u = 0.55$ m/s) demonstrating a smaller value of t_0 than the sparser Outdoor data set ($\rho = 0.27$ m^{-2}, $u = 0.86$ m/s) [37]. While the large-τ behavior in our data sets is therefore dominated by screening, we can use the largest observed values of t_0 to place a lower bound estimate on the intrinsic range of unscreened interactions (which we denote as τ_0). This estimate suggests that an appropriate value is $\tau_0 \approx 3$ s, which is consistent with previous research demonstrating an interaction time horizon of 2–4 s [21].

Since the interaction energy follows a power law with a sharp truncation at large τ, we infer from the data the following form of the pedestrian interaction law:

$$E(\tau) = \frac{k}{\tau^2} e^{-\tau/\tau_0}. \tag{2}$$

Here, k is a constant that sets the units for energy.

To demonstrate the general nature of the identified interaction law, we performed simulations of pedestrians that adapt their behavior according to Eq. (2) via force-based interactions. In particular, the energy $E(\tau)$ directly implies a natural definition of the force **F** experienced by pedestrians when interacting:

$$\mathbf{F} = -\nabla_\mathbf{r} \left(\frac{k}{\tau^2} e^{-\tau/\tau_0} \right), \tag{3}$$

where $\nabla_\mathbf{r}$ is the spatial gradient. A full analytical expression for this derivative is given in the Supplemental Material [29].

For the purposes of simulation, each pedestrian is also given a driving force associated with its desired direction of motion, following Ref. [9]. The resulting force model is sufficient to reproduce a wide variety of important pedestrian behaviors, including the formation of lanes, arching in narrow passages, slowdowns in congestion, and anticipatory collision avoidance (Fig. 3). Additionally, the simulated pedestrians match the known *fundamental diagram* [38] of speed-density relationships for real human crowds and qualitatively capture the empirical behavior of $g(r)$ depicted in Fig. 1(c) [29].

Our simulations also reproduce the anticipatory power law described by Eq. (2), as shown in Fig. 4. In contrast, simulations generated by distance-based interaction forces fail to show a dependence of E on τ (Fig. 4, inset). Other, more recent models of pedestrian behavior also cannot consistently capture the empirical power-law relationship (see the Supplemental Material [29]). The ability of our own simulations to reproduce $E(\tau)$ also provides a self-consistent
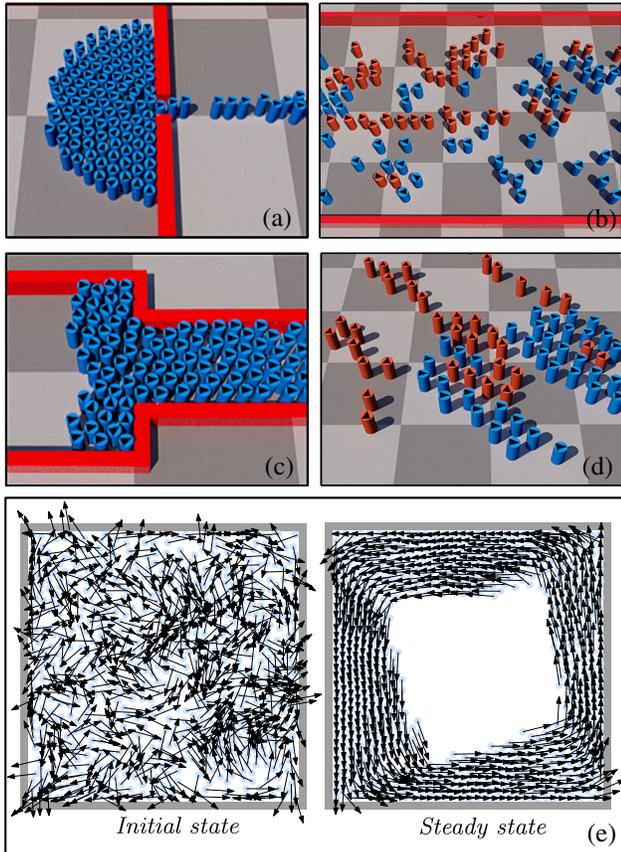
FIG. 3 (color online). Stills from simulations of agents following the force law derived from Eq. (2). In panels (a)–(d), agents are represented as cylinders and color coded according to their goal direction. The simulated agents display many emergent phenomena also seen in human crowds, including arching around narrow passages (a), clogging and "zipping" patterns at bottlenecks (c), and spontaneously self-organized lane formation (b) and (d). Panel (e) depicts a simulation of agents without a preferred goal direction (arrows represent the agents' current orientations). The agents' interactions lead to large-scale synchronization of their motion. Further simulation details are given in the Supplemental Material [29].

FIG. 4 (color online). Inferred interaction energy $E \propto \ln(1/g)$ as a function of time to collision τ for different simulations, obtained using the anticipatory force described by Eq. (3), and the distance-dependent force described in Ref. [9] (inset). For simulations with strictly distance-dependent interactions, the inferred interaction energy does not show a dependence on τ. In contrast, simulations following our model closely match the observed empirical power law for $E(\tau)$. Shaded regions denote average energy values ± 1 standard deviation.

A detailed study of such collective behaviors, however, is outside the scope of our present work.

While the model implied by Eq. (3) is widely applicable, it may not be sufficient on its own to capture certain crowd phenomena, such as the shock waves and turbulent flows that have been reported to occur in extremely high density crowds [46]. In such very dense situations, saturating effects such as finite human reaction time become relevant, and these may alter the quantitative form of the interaction in a way that is not well-captured by our time-to-collision-based analysis. Augmenting our result with an additional close-ranged component of the interaction may give a better description of these extremely dense scenarios, and is a promising avenue for future work.

To conclude, our statistical mechanics-based analysis of a large collection of human data has allowed us to quantify the nature and strength of interactions between pedestrians. This novel type of analysis opens new avenues for studying the behavior of humans using real life data. The data we have analyzed here reveal the existence of a single anticipatory power law governing the motions of humans. The consistency of this law across a variety of scenarios provides a new means to understand how pedestrians behave and suggests new ways to evaluate models of pedestrian interactions. Further, these results suggest a general quantitative law for describing human anticipation that may extend to other studies of human behavior, which may therefore be amenable to a similar type of analysis.

See Ref. [47] for information regarding simulation source code and videos.

validation of our use of the Boltzmann relation to infer the interaction energy from data.

Interesting behavior can also be seen when Eq. (3) is applied to walkers propelled forward in the direction of their current velocity without having a specific goal (as implemented, for example, in Ref. [39]). In such cases, complex spatiotemporal patterns emerge, leading eventually to large-scale synchronization of motion. An example is illustrated in Fig. 3(e), where a collection of pedestrians that is initialized to a high energy state with many imminent collisions settles over time into a low energy state where pedestrians move in unison. This result is qualitatively similar to observed behavior in dense, non-goal-oriented human crowds [40], and is reminiscent of the "flocking" behavior seen in a variety of animal groups [41–45].

———————

[1] D. Helbing, P. Molnár, I. Farkas, and K. Bolay, Environ. Plann. B **28**, 361 (2001).

[2] M. Moussaïd, E. G. Guillot, M. Moreau, J. Fehrenbach, O. Chabiron, S. Lemercier, J. Pettré, C. Appert-Rolland, P. Degond, and G. Theraulaz, PLoS Comput Biol. **8**, e1002442 (2012).

[3] W. Yu and A. Johansson, Phys. Rev. E **76**, 046105 (2007).

[4] D. Helbing, Rev. Mod. Phys. **73**, 1067 (2001).

[5] L. P. Kadanoff, J. Stat. Phys. **39**, 267 (1985).

[6] S. Hoogendoorn and P. H. L. Bovy, Transp. Res. Rec. **1710**, 28 (2000).

[7] R. Hughes, Transportation Research, Part B (Methodological) **36**, 507 (2002).

[8] A. Kirchner, K. Nishinari, and A. Schadschneider, Phys. Rev. E **67**, 056122 (2003).

[9] D. Helbing, I. Farkas, and T. Vicsek, Nature (London) **407**, 487 (2000).

[10] W. J. Yu, R. Chen, L. Y. Dong, and S. Q. Dai, Phys. Rev. E **72**, 026112 (2005).

[11] M. Chraibi, A. Seyfried, and A. Schadschneider, Phys. Rev. E **82**, 046111 (2010).

[12] S. Hoogendoorn and P. H. L. Bovy, Optimal Control Applications and Methods **24**, 153 (2003).

[13] M. Moussaïd, D. Helbing, S. Garnier, A. Johansson, M. Combe, and G. Theraulaz, Proc. R. Soc. B **276**, 2755 (2009).

[14] B. R. Fajen and W. H. Warren, J. Exp. Psychol. **29**, 343 (2003).

[15] C. W. Reynolds, ACM Comput. Graph. **21**, 25 (1987).

[16] D. Helbing and P. Molnár, Phys. Rev. E **51**, 4282 (1995).

[17] M. Gérin-Lajoie, C. Richards, and B. McFadyen, Motor Control **9**, 242 (2005).

[18] T. Ducourant, S. Vieilledent, Y. Kerlirzin, and A. Berthoz, Neurosci. Lett. **389**, 6 (2005).

[19] A. Johansson, Phys. Rev. E **80**, 026120 (2009).

[20] L. Noy, E. Dekel, and U. Alon, Proc. Natl. Acad. Sci. U.S.A. **108**, 20947 (2011).

[21] A.-H. Olivier, A. Marin, A. Crétual, and J. Pettré, Gait Posture **36**, 399 (2012).

[22] J. Ondřej, J. Pettré, A.-H. Olivier, and S. Donikian, ACM Trans. Graph. **29**, 1 (2010).

[23] F. Zanlungo, T. Ikeda, and T. Kanda, Europhys. Lett. **93**, 68005 (2011).

[24] M. Moussaïd, D. Helbing, and G. Theraulaz, Proc. Natl. Acad. Sci. U.S.A. **108**, 6884 (2011).

[25] S. J. Guy, S. Curtis, M. C. Lin, and D. Manocha, Phys. Rev. E **85**, 016110 (2012).

[26] A. Lerner, Y. Chrysanthou, and D. Lischinski, Computer Graphics Forum **26**, 655 (2007).

[27] S. Pellegrini, A. Ess, K. Schindler, and L. Van Gool, in *IEEE International Conference on Computer Vision* (IEEE, Piscataway, NJ, 2009), pp. 261–268.

[28] A. Seyfried, O. Passon, B. Steffen, M. Boltes, T. Rupprecht, and W. Klingsch, Transp. Sci. **43**, 395 (2009).

[29] See the Supplemental Material at http://link.aps.org/supplemental/10.1103/PhysRevLett.113.238701, which includes Refs. [30–34], for experimental data sets, statistical methods, a simulation model derived from our law, and simulation results.

[30] A. Seyfried, M. Boltes, J. Kähler, W. Klingsch, A. Portz, T. Rupprecht, A. Schadschneider, B. Steffen, and A. Winkens, in *Pedestrian and Evacuation Dynamics 2008*, edited by W. Klingsch, C. Rogsch, A. Schadschneider, and M. Schreckenberg (Springer, Berlin, 2010) pp. 145–156.

[31] M. Boltes, A. Seyfried, B. Steffen, and A. Schadschneider, in *Pedestrian and Evacuation Dynamics 2008*, edited by W. Klingsch, C. Rogsch, A. Schadschneider, and M. Schreckenberg (Springer, Berlin, 2010) pp. 43–54.

[32] L. C. Edie, in *Proceedings of the Second International Symposium on the Theory of Traffic Flow: London 1963* (OECD, Paris, France, 1965), pp. 139–154.

[33] S. P. Hoogendoorn and W. Daamen, Transp. Sci. **39**, 147 (2005).

[34] S. Hoogendoorn and W. Daamen, in *Traffic and Granular Flow '03* (Springer, Berlin, 2005) pp. 373–382.

[35] G. D. Mahan, *Many-Particle Physics* (Plenum, New York, 1990).

[36] M. Babadi, B. Skinner, M. M. Fogler, and E. Demler, Europhys. Lett. **103**, 16002 (2013).

[37] The ratio of $(\rho^{-1/2})/u$ between the Bottleneck and Outdoor data sets is $(1.15\,\text{s})/(2.25\,\text{s}) = 0.51$. For comparison, the measured values of t_0 have a ratio $(1.4\,\text{s})/(2.4\,\text{s}) = 0.58$.

[38] U. Weidmann, *Transporttechnik der Fußgänger*, Literature Research, Vol. 90 (ETH Zürich, 1993).

[39] D. Grossman, I. S. Aranson, and E. B. Jacob, New J. Phys. **10**, 023036 (2008).

[40] J. L. Silverberg, M. Bierbaum, J. P. Sethna, and I. Cohen, Phys. Rev. Lett. **110**, 228701 (2013).

[41] T. Vicsek, A. Czirók, E. Ben-Jacob, I. Cohen, and O. Shochet, Phys. Rev. Lett. **75**, 1226 (1995).

[42] I. D. Couzin, J. Krause, R. James, G. D. Ruxton, and N. R. Franks, J. Theor. Biol. **218**, 1 (2002).

[43] M. Ballerini, N. Cabibbo, R. Candelier, A. Cavagna, E. Cisbani, I. Giardina, V. Lecomte, A. Orlandi, G. Parisi, A. Procaccini, M. Viale, and V. Zdravkovic, Proc. Natl. Acad. Sci. U.S.A. **105**, 1232 (2008).

[44] I. L. Bajec and F. H. Heppner, Animal Behaviour **78**, 777 (2009).

[45] T. Vicsek and A. Zafeiris, Phys. Rep. **517**, 71 (2012).

[46] D. Helbing, A. Johansson, and H. Z. Al-Abideen, Phys. Rev. E **75**, 046109 (2007).

[47] Complete simulation source code, along with videos and links to data used in this study, can be found at our companion webpage: http://motion.cs.umn.edu/PowerLaw.